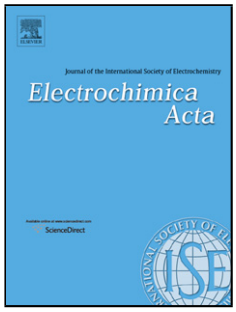

Title: Soluble tetratriphenylamine Zn phthalocyanine as Hole Transporting Material for Perovskite Solar Cells

Author: Esmaiel Nouri Jonnadula Venkata Suman Krishna Challuri Vijay Kumar Vassilios Dracopoulos Lingamallu Giribabu Mohammad Reza Mohammadi Panagiotis Lianos

PII: S0013-4686(16)32382-9
DOI: http://dx.doi.org/doi:10.1016/j.electacta.2016.11.052
Reference: EA 28342

To appear in: *Electrochimica Acta*

Received date: 22-9-2016
Revised date: 2-11-2016
Accepted date: 9-11-2016

Please cite this article as: Esmaiel Nouri, Jonnadula Venkata Suman Krishna, Challuri Vijay Kumar, Vassilios Dracopoulos, Lingamallu Giribabu, Mohammad Reza Mohammadi, Panagiotis Lianos, Soluble tetratriphenylamine Zn phthalocyanine as Hole Transporting Material for Perovskite Solar Cells, Electrochimica Acta http://dx.doi.org/10.1016/j.electacta.2016.11.052

Soluble tetratriphenylamine Zn phthalocyanine as Hole Transporting Material for Perovskite Solar Cells.

Esmaiel Nouri[a+], Jonnadula Venkata Suman Krishna[b], Challuri Vijay Kumar[c++], Vassilios Dracopoulos[c], Lingamallu Giribabu[b]*, Mohammad Reza Mohammadi[d], Panagiotis Lianos[a]*

[a]Department of Chemical Engineering, University of Patras, 26500 Patras, Greece

[b]Inorganic and Physical Chemistry Division, Indian Institute of Chemical Technology, Hyderabad, 500 007 India.

[c]FORTH/ICE-HT, P.O. Box 1414, 26504 Patras, Greece

[d]Department of Materials Science and Engineering, Sharif University of Technology, Azadi Str., Tehran, Iran

[+]Permanent Address: Department of Materials Science and Engineering, Sharif University of Technology, Azadi Str., Tehran, Iran

[++] Present Address: Laboratoire de Réactivité et Chimie des Solides, Université de Picardie Jules Verne, CNRS UMR 7314, 33 rue Saint Leu, Amiens 80039, France

CORRESPONDING AUTHORS: giribabu@iict.res.in and lianos@upatras.gr

Graphical Abstract

For the manuscript EO16-1873: "Soluble tetratriphenylamine Zn phthalocyanine as Hole Transporting Material for Perovskite Solar Cells".

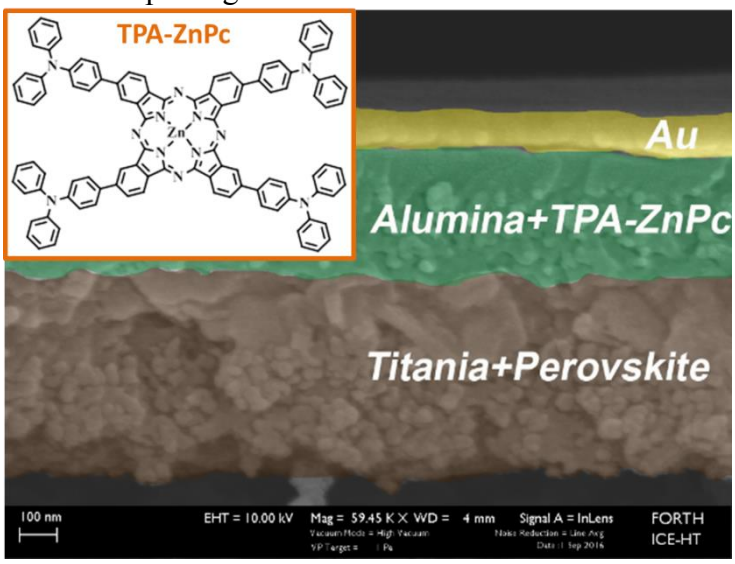

Highlights

for the manuscript EO16-1873: "Soluble tetratriphenylamine Zn phthalocyanine as Hole Transporting Material for Perovskite Solar Cells".

- New hole transporting material for perovskite solar cells based on metal phthalocyanine core
- Soluble tetratriphenylamine Zn phthalocyanine employed for this purpose shows good functionality
- Importance of the presence of Al_2O_3 as buffer layer

Abstract

Perovskite solar cells have been constructed under the standard procedure by employing soluble tetratriphenylamine-substituted Zn phthalocyanine as hole transporting material. Solution processed device construction was carried out under ambient conditions of 50-60% ambient humidity. Triphenylamine substitution played the double role of imparting solubility to the core metal phthalocyanine as well as to

introduce electron-rich ligands, which could enhance the role of Zn phthalocyanine as hole transporter. Indeed, the obtained material was functional. The present data highlight tetratriphenylamine-substituted Zn phthalocyanine as hole transporting material but also highlight the importance of the presence of a buffer layer between the perovskite layer and the hole-transporting layer. Thus the efficiency of the cells was 9.0% in the absence but increased to 13.65% in the presence of Al_2O_3 buffer layer.

Key words: perovskite; solar cells; hole transport material; phthalocyanine.

1. Introduction

Perovskite solar cells (PSCs) have established themselves as the most promising next generation photovoltaics. In their most common version, PSCs are composed of a layer structure formed on a transparent electrode and made of a thin layer of nanoparticulate titania, an organometal halide perovskite layer, an organic hole transporting layer (HTL) and a top gold electrode. One of the crucial components of PSCs is the HTL, which is made by thin film deposition of a hole conductor. The standard hole conductor is 2,2',7,7'-Tetrakis-(N,N-di-4-methoxyphenylamino)-9,9'-spirobifluorene (spiro-OMeTAD). This material has raised skepticism as to its complexity and cost of synthesis as well as to its stability and conductivity **[1-4]**. For this reason, other possible hole transporting materials (HTMs) have been recently intensively studied. One group of HTMs is that of metal phthalocyanines **[5-11]**. Metal phthalocyanines have been broadly studied as sensitizers for dye-sensitized

solar cells **[12-14]**, as components for organic photovoltaics **[15, 16]** as well as for other photonic applications **[17-19]**. Metal phthalocyanines are very stable materials so that in their insoluble version they may be deposited by thermal evaporation **[5, 7]**. For several practical purposes, it is preferable to use metal phthalocyanines which are soluble in volatile organic solvents thus allowing solution processed device construction. It has been, for example, previously shown **[8]** that tetra n-butyl substituted copper phthalocyanine (CuPc) not only makes a soluble material but the presence of flexible n-butyl chains facilitates molecular packing and π-π interaction that ensures sufficient electrical conductivity. A soluble ZnPc was also obtained by octa(2,6-diphenylphenoxy) substitution and presented in ref. **[9]**. In that case, the focus was placed on an effort to avoid parent molecule aggregation, which is a common problem with metal Pc. Improvement of soluble ZnPc properties as HTM has lately been achieved by diphenylamino substitution **[10]**, where it was shown that ZnPc bearing electron rich bis-aryl substituents can effectively enhance material's performance as HTM. Motivated by these data, in the present work we have tested the possibility to enhance ZnPc functionality by tetratriphenylamine substitution (TPA-ZnPc), i.e. by introducing another electron rich substituent, which also imparts solubility and allows solution processed device fabrication.

2. Experimental

2.1 Materials

All materials were purchased from Aldrich, unless otherwise specified, and were used as received. Fluorine doped SnO_2 (FTO) glasses of 8 ohm/square were purchased from Pilkington.

2.2 Synthesis of 4,4'-Diphenylamino-biphenyl-3,4-dicarbonitrile

This ligand was synthesized according to the literature reported procedure **[20]** (see **Figure1**).

2.3 Synthesis of TPA-ZnPc

A mixture of anhydrous zinc acetate (1.90 g, 10 mmol), 4,4'-Diphenylamino-biphenyl-3,4-dicarbonitrile (1.70 g, 5 mmol), 1,8-Diazabicyclo[5.4.0] undec-7-ene (DBU, catalytic amount) and dry 1-pentanol (5 ml) was refluxed at 150 ºC for 16 h under a nitrogen atmosphere. After cooling, the solution was precipitated by addition of methanol, filtered and dried. The obtained solid material was subjected to silica gel column chromatography and eluted with dichloromethane. The green coloured band was collected and recrystallized from methanol, to get the desired compound in 70% yield. Elemental analysis of Anal. Calcd. for $C_{104}H_{68}N_{12}Zn$% (1551.11): C, 80.53; H, 4.42; N, 10.84. Found: C, 80/50; H, 4.43; N, 10.80. MALDI-TOF: $C_{104}H_{68}N_{12}Zn$ m/z: 1550 (calcd. for $[M]^+$). ^1H NMR (500 MHz, $CDCl_3$): δ 7.68 – 7.63 (m, 4H), 7.55 - 7.54 (d, *J* = 8.3 Hz, 8H), 7.45 (s, 8H), 7.43 (d, *J* = 1.7 Hz, 8H), 7.35 – 7.29 (m, 40H). FT-IR (KBr) ν_{max} 3030, 2922, 1278 and 1099 cm^{-1}.

2.4 Fabrication of perovskite solar cell devices

FTO-coated glass substrates were cut in pieces of dimensions 1 cm ×3 cm. One third of the conductive layer was removed using zinc powder and hydrochloric acid. Then they were washed with mild detergent, rinsed several times with distilled water and subsequently with ethanol and acetone in an ultrasonic bath, finally dried under air stream. A compact thin layer of TiO_2 was then deposited on this patterned and cleaned FTO electrode by aerosol spray pyrolysis using a solution of 0.2 M diisopropoxytitanium bis(acetylacetonate) in EtOH. After spraying, the samples were

heated for 1 h at 500 ˚C. Subsequently, a mesoporous TiO_2 layer composed of titania paste made of P25 nanoparticles was spin coated at 4000 rpm for 60 s and then dried at 100 ˚C for 20 min and calcined for 30 min at 500 ˚C. After that, the samples were treated in $TiCl_4$ by dipping into a solution made of 0.04 M $TiCl_4$ in H_2O for 30 min at 70 ˚C, then copiously rinsing and finally calcining at 500 ˚C. Active perovskite layer was deposited on the titania film by the following procedure. A precursor solution was made by mixing 253 mg $PbCl_2$ and 507 mg PbI_2 with 270 mg methyl ammonium iodide in 1.5 ml dimethylsulfoxide (DMSO). The solution was kept under stirring for about 2 h at about 80 ˚C and then deposited in two consecutive spin-coating steps by applying the anti-solvent technique: first 1000 rpm for 10 s, then 6000 rpm for 30 s. During the second step, 1 mL chlorobenzene, as anti-solvent, was gently dropped on the spinning substrate. The layer was then heated at 90 ˚C for about 45 min, which made the sample's color turn from yellow to black. Thereafter, a thin mesoporous Al_2O_3 buffer layer was spin-coated directly on the annealed perovskite layer at 2000 rpm for 60 s. For this purpose, we used a colloidal dispersion of aluminum oxide (Al_2O_3) nanoparticles (<50 nm particle size, 20 wt.% in isopropanol), which was further diluted by sonicating 200 µL of the original dispersion in 2 mL isopropanol. TPA-ZnPc as hole transporting material (HTM) was then deposited by spin coating at 3000 rpm for 60 s. The TPA-ZnPc solution was prepared by dissolving 40 mg of TPA-ZnPc powder in 1 ml of chlorobenzene at 50 °C. In this solution we added 28.8 µL of 4-tert-butylpyridine (TBP) and 17.5 µL of a stock solution of lithium bis(trifluoromethane sulfonyl) imide (Li-TFSI) in acetonitrile (520 mg/1 mL). All of these procedures were carried out under ambient conditions of 50–60 % relative humidity. The last step for preparing the solid state solar cell was the deposition of ≈ 90 nm thick gold electrodes by thermal evaporation under vacuum. The thickness of

the subsequent layers forming the solar cells can be seen in the FESEM cross-sectional image of **Figure 2**. The unit devices had an active size of 15 mm^2 (10 mm × 1.5 mm) as defined by the size of the gold electrodes.

2.5 Characterizations

Illumination of the solar cells was made with a PECCELL PEC-L01 Solar Simulator set at 100 mW/cm^2, through a mask of aperture size 1×6 mm^2. J–V characteristic curves were recorded under ambient conditions with a Keithley 2601 source meter that was controlled by Keithley computer software (LabTracer). IPCE values were obtained with an Oriel IQE 200 system. Absorption and photoluminescence spectra using thin transparent perovskite films were recorded with a Cary 1E UV-Vis spectrophotometer and a Cary Eclipse Fluorescence spectrometer, respectively. Impedance spectroscopy (IS) was carried out on PSC devices using an Autolab PGSTAT 128N potentiostat. Finally, FESEM measurements were made using a Zeiss SUPRA 35VP microscope.

3. Results and discussion

Figure 3 shows absorption spectra of a dilute solution (Curve 1) and thin film (Curve 2) of TPA-ZnPc. The dilute-solution spectrum gives a fine spectral structure with emphasis on the longer wavelength peak of the Q-band (Curve 1). When TPA-ZnPc was deposited as thin film on an FTO substrate (Curve 2) an extensive broadening of the Q band revealed strong molecular packing. Molecular packing is necessary in order to ensure π-π interaction and sufficient electrical conductivity.

TPA-ZnPc films were deposited on the top of the perovskite layer as HTM, alone or with the intermediate of a Al_2O_3 buffer layer. Such buffer layers are a

common practice in the construction of of PSCs. Al_2O_3 is a standard choice for this purpose **[21]**. Moreover, SiO_2 **[22]**, montmorillonite **[23]**, ZrO_2 **[24]**, ZnO **[25]**, glycerol-doped PEDOT:PSS **[26]**, LiF and C_{60} **[27]** are further examples of buffer layer for solid-state solar cells. The buffer layer plays a multiple role in solar cell functionality. The simplest and most effective one is that its presence discourages the formation of shunt paths towards both electrodes, which may result in a decrease of shunt resistance and thus a drop in fill factor (FF) and open-circuit voltage (V_{OC}) of the cell **[21-25,28]**. The buffer layer also prevents any corrosive additives employed with HTM to reach and destroy the perovskite layer **[23]**. Furthermore, it provides a porous framework, which organizes the formation of the upper HTM layer, facilitating proper film formation even in a case of a hardly soluble and hardly processable HTM **[9,21]**. By improving the formation of the HTM layer, it facilitates hole transfer and conduction and limits charge recombination **[21-23,26]**. It can also improve the stability of the PSCs **[27]**. Thus in the present case we emloyed the standard Al_2O_3 buffer layer, which once more proved itself beneficial to cell performance, as will be shown by the following data. **Figure 4** shows the FESEM top views of the TPA-ZnPc films without (a) and with an underlying Al_2O_3 layer (b). TPA-ZnPc film alone formed a structure with pinholes. However, in the presence of Al_2O_3 the structure attained a fully-covered compact structure without such holes. Obviously, the presence of the buffer layer may serve, among other functions, to block such voids and thus block shunt paths.

The cross sectional FESEM image of a typical PSC device is shown in **Figure 2**. The presence of the Al_2O_3 buffer layer induces a thicker hole transporting layer (**Figure 2b**) in comparison with neat TPA-ZnPc (**Figure 2a**). By controlling the spin-coating speed we obtained Al_2O_3 buffer layer films of various thicknesses. The one

shown in **Figure 2b** gave optimal results, in terms of cell efficiency. This is in accordance with literature data indicating that a layer about 200 nm thick offers optimal results **[29].**

The performanance of the PSCs made with TPA-ZnPc as HTL with or without an intermediate buffer layer is presented by the current-voltage data of **Figure 5.** Curves were ploted in forward and reverse recording in order to demonstrate any hysterisis effect. The results suggest that the hysteresis in the present devices was small. The beneficial effect produced in the presence of the buffer layer is obvious. All three photovoltaic parameters (J_{SC}, FF and V_{OC}) remarkably increased and this resulted in a large increase of the cell efficiency, which changed from 9.0% to 13.65%. Increase of the fill factor and of the open-circuit voltage are standard indicators of blocking of the shunt paths across the cell and this was presently attained in the presence of the Al_2O_3 buffer layer. An improvement of J_{SC} from 16 to 20 mA/cm^2 has also been observed. The enhancement of J_{SC} in PSCs was further evidenced by the modification in the action spectra of **Figure 6**.

Additional functionalities of the Al_2O_3 buffer layer as blocking layer are also highlighted by the data of **Figure 7**. A perovskite film has been deposited on plain glass and its absorption and photoluminescence spectra have been recorded. Organometal halide perovskites emit substantial photoluminescence. Then on the top of the perovskite film a layer of TPA-ZnPc was deposited with or without an intermediate Al_2O_3 buffer layer. In the presence of TPA-ZnPc, the luminescence was extensively quenched, suggesting its efficient hole scavenging. It is interesting to note that quenching was even more extensive in the presence of the buffer layer. The results of **Figure 7** highlight TPA-ZnPc as efficient hole scavenger but they also highlight Al_2O_3 as a means to further facilitate this functionality. Thus, we can

conclude that the buffer layer can efficiently suppress charge recombination in the PSCs.

To get further insights on the charge transport properties of the TPA-ZnPc in PSCs, we also performed impedence spectroscopy measurements, as shown in **Figure 8**. It is noticed that the Al_2O_3 buffer layer not only formed a blocking layer, but also retarded the charge recombination. The Nyquist plot of impedance spectra in the dark under V_{OC} bias voltage revealed a slight increase in the recombination resistance (**Figure 8a**). Generally, an increased resistance in the dark indicates restrained electron recombination **[30]**. Under illumination conditions (**Figure 8b**), the recombination resistance further increased, much more than in the dark.

Conclusions

Soluble tetratriphenylamine substituted Zn phthalocyanine, TPA-ZnPc, functions as a HTL in perovskite solar cells. TPA-ZnPc offers a substantial cell efficiency, which is increased by more than 50% when an alumina buffer layer is introduced between the perovskite and the hole transporting layer. The present work highlights TPA-ZnPc as a HTM for perovskite solar cells and also highlights the importance of the intermediate buffer layer. This layer assists better HTM film formation and discourages electron-hole recombination.

Acknowledgements

M.R. Mohammadi and E. Nouri wish to thank the financial support by Sharif University of Technology through research grant no. G940309, and especially the financial support by Iran National Science Foundation (INSF).

References

[1] S. Ameen, M. A. Rub, S. A. Kosa, K. A. Alamry, M. S. Akhtar, H. S. Shin, H. K. Seo, A. M. Asiri, M. K. Nazeeruddin, Perovskite Solar Cells: Influence of Hole Transporting Materials on Power Conversion Efficiency, ChemSusChem 9 (2016) 10–27.

[2] F.Bella, G.Griffini, J.-P. Correa-Baena, G.Saracco, M.Gratzel, A.Hangfeldt, S.Turri,C.Gerrbaldi, Improving efficiency and stability of perovskite solar cells with photocurable fluoropolymers, Science 354 (2016) 203-206.

[3] A.K.Baranwal, S.Kanaya, T.A.Peiris, G.Mizuta, T.Nishina, T.Miyasaka, H.Segawa, S.Ito, 100 °C Thermal Stability of Printable Perovskite Solar Cells Using Porous Carbon Counter Electrodes, ChemSusChem 9 (2016) 2604-2608.

[4] F.Bella, Polymer electrolytes and perovskites: lights and shadows in photovoltaic devices, Electrochimica Acta 175 (2015) 151–161

[5] C. V. Kumar, G. Sfyri, D. Raptis, E. Stathatos, P. Lianos, Perovskite Solar Cell with Low Cost Cu-Phthalocyanine as Hole Transporting Material, RSC Adv., 5 (2015) 3786–3791.

[6] G. Sfyri, C. V. Kumar, G. Sabapathi, L. Giribabu, K. S. Andrikopoulos, E. Stathatos, P. Lianos, Subphthalocyanine as Hole Transporting Material for Perovskite Solar Cells, RSC Adv., 5 (2015) 69813–69818.

[7] G. Sfyri, C. V. Kumar, Y. L. Wang, Z. X. Xu, C. A. Krontiras, P. Lianos, Tetra Methyl Substituted Cu(II) Phthalocyanine as Alternative Hole Transporting Material for Organometal Halide Perovskite Solar Cells, Appl. Surf. Sci., 360 (2016) 767–771.

[8] G.Sfyri, Q.Chen, Y.-W.Lin, Y.-L.Wang, E.Nouri, Z.-X.Xu, P.Lianos, Soluble butyl substituted copper phthalocyanine as alternative hole-transporting material for solution processed perovskite solar cells, Electrochimica Acta, 212 (2016) 929–933.

[9] F. J. Ramos, M. Ince, M. Urbani, A. Abate, M. Gratzel, S. Ahmad, T. Torres, M. K. Nazeeruddin, Non-aggregated Zn(II) Octa(2,6-diphenylphenoxy) Phthalocyanine as a Hole Transporting Material for Efficient Perovskite Solar Cells, Dalton Trans., 44 (2015) 10847–10851.

[10] K.T. Cho, K. Rakstys, M. Cavazzini, S. Orlandi, G. Pozzi, M.K. Nazeeruddin, Perovskite Solar Cells Employing Molecularly Engineered Zn(II) Phthalocyanines as Hole-transporting Materials, Nano Energy, in press.

[11] W. Ke, D. Zhao, C.R. Grice, A.J. Cimaroli, G. Fang, Y. Yan, Efficient fully-vacuum-processed perovskite solar cells using copper phthalocyanine as hole selective layers, J. Mater. Chem. A, 3 (2015) 23888–23894.

[12] M. Ince, J.H. Yum, Y. Kim, S. Mathew, M. Grätzel, T. Torres, M.K. Nazeeruddin, Molecular Engineering of Phthalocyanine Sensitizers for Dye-Sensitized Solar Cells. J. Phys. Chem. C, 118 (2014) 17166–17170.

[13] L. Tejerina, M.V. Martínez-Díaz, M.K. Nazeeruddin, T. Torres, The Influence of Substituent Orientation on the Photovoltaic Performance of Phthalocyanine-Sensitized Solar Cells, Chem. Eur. J., 22 (2016) 4369–4373.

[14] V.K. Singh, R.K. Kanaparthi, L. Giribabu, Emerging Molecular Design Strategies of Unsymmetrical Phthalocyanines for Dye-Sensitized Solar Cell Applications, RSC Adv., 4 (2014) 6970-6984.

[15] Y. Zhang, Z. Wei, Enhancing the Performance of Polymer Solar Cells Using CuPc Nanocrystals as Additives, Nanotechnology, 26 (2015) 204001.

[16] D. Qu, R. Guo, S. Yue, Y. Wu, P. Yan, G. Cheng, Planar Heterojunction Organic Photovoltaic Cells Based on Tetramethyl Substituted Copper(II) Phthalocyanine Treated with Thermal Annealing, J. Phys. D: App. Phys., 47 (2014) 415104.

[17] J. Xu, Y. Wang, H. Shan, Y. Lin, Q. Chen, V.A.L. Roy, Z. Xu, Ultrasound-Induced Organogel Formation Followed by Thin Film Fabrication via Simple Doctor Blading Technique for Field-Effect Transistor Applications, ACS Appl. Mater. Interfaces, 8 (2016) 18991–18997.

[18] J. Xu, Y. Wang, Q. Chen, Y. Lin, H. Shan, V. A. L. Roy, Z. Xu, Enhanced Lifetime of Organic Light-Emitting Diodes Using Soluble Tetraalkyl-Substituted Copper Phthalocyanines as Anode Buffer Layers, J. Mater. Chem. C, 4 (2016) 7377–7382.

[19] D. Swain, V.K. Singh, N.V. Krishna, L. Giribabu, S.V. Rao, Optical, Electrochemical, Third-Order Nonlinear Optical, and Excited State Dynamics Studies of Thio-Zinc Phthalocyanine, J. Porphyrins Phthalocyanines 18 (2014) 305–315.

[20] L. Giribabu, V.K. Singh, C.V. Kumar, Y. Soujanya, P.Y. Reddy, and M.L. Kantam, Triphenylamine–phthalocyanine based sensitizer for sensitization of nanocrystalline TiO_2 films. Solar Energy, 85(2011)1204-1212.

[21] S. Guarnera, A. Abate, W. Zhang, J.M. Foster, G. Richardson, A. Petrozza, H.J. Snaith, Improving the Long-Term Stability of Perovskite Solar Cells with a Porous Al_2O_3 Buffer-Layer, J Phys Chem Lett., 6 (2015) 432–437.

[22] S.K. Pathak, A. Abate, T. Leijtens, D.J. Hollman, J. Teuscher, L. Pazos, P. Docampo, U. Steiner, H.J. Snaith, Towards Long-Term Photostability of

Solid-State Dye Sensitized Solar Cells, Adv. Energy Mater., 4 (2014) 1301667(1-9).

[23] W. Li, H. Dong, L. Wang, N. Li, X. Guo, J. Li, Y. Qiu, Montmorillonite as Bifunctional Buffer Layer Material for Hybrid Perovskite Solar Cells with Protection from Corrosion and Retarding Recombination, J. Mater. Chem. A, 2 (2014) 13587–13592.

[24] C.Y. Chang, W.K. Huang, J.L. Wu, Y.C. Chang, K.T. Lee, C.T. Chen, Room-temperature Solution-Processed n-Doped Zirconium Oxide Cathode Buffer Layer for Efficient and Stable Organic and Hybrid Perovskite Solar Cells, Chem. Mater., 28 (2016) 242–251.

[25] X. Jia, L. Zhang, Q. Luo, H. Lu, X. Li, Z. Xie, Y. Yang, Y. Q. Li, X. Liu, C.Q. Ma, Power Conversion Efficiency and Device Stability Improvement of Inverted Perovskite Solar Cells by Using a ZnO:PFN Composite Cathode Buffer Layer, ACS Appl. Mater. Interfaces, 8 (2016)18410–18417.

[26] J.F. Li, C. Zhao, H. Zhang, J.F. Tong, P. Zhang, C.Y. Yang, Y.J. Xia, D.W. Fan, Improving the performance of perovskite solar cells with glycerol-doped PEDOT:PSS buffer layer, Chin. Phys. B, 25 (2016) 028402 (1–5).

[27] X. Liu, H. Yu, L. Yan, Q. Dong, Q. Wan, Y. Zhou, B. Song, Y. Li, Triple Cathode Buffer Layers Composed of PCBM, C60 and LiF for High Performance Planar Perovskite Solar Cells, ACS Appl. Mater. Interfaces, 7 (2015) 6230–6237.

[28] C.Y. Chang, W.K. Huang, J.L. Wu, Y.C. Chang, K.T. Lee, C.T. Chen, Room-Temperature Solution-Processed n-Doped Zirconium Oxide Cathode Buffer Layer for Efficient and Stable Organic and Hybrid Perovskite Solar Cells, Chem. Mater., 28 (2016) 242–251.

[29] N.Marinova, W.Tress, R.Humphry-Baker, M.I.Dar, V.Bojinov, S.M.Zakeeruddin, M.K.Nazeeruddin, Michael Grätzel, Light Harvesting and Charge Recombination in CH3NH3PbI3 Perovskite Solar Cells Studied by Hole Transport Layer Thickness Variation, ACS Nano, 9 (2015) 4200–4209.

[30] A. Dualeh, T. Moehl, N. Tetreault, J. Teuscher, P. Gao, M.K. Nazeeruddin, M. Gratzel, Impedance Spectroscopic Analysis of Lead Iodide Perovskite-Sensitized Solid-State Solar Cells, ACS Nano, 8 (2014) 362–373.

Figure Captions

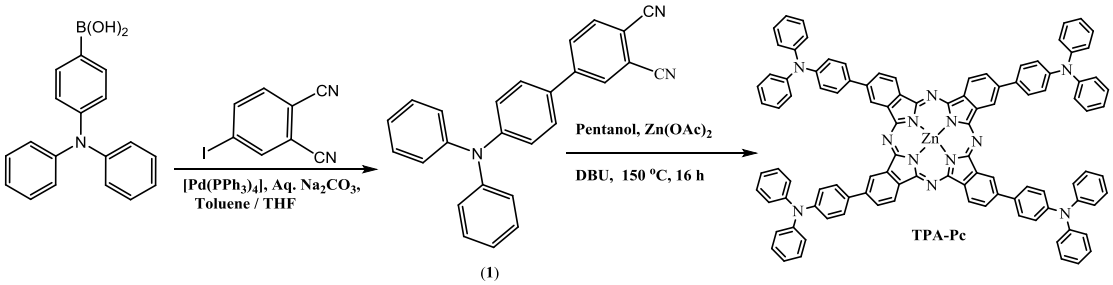

Figure 1. *Synthesis scheme for TPA-ZnPc.*

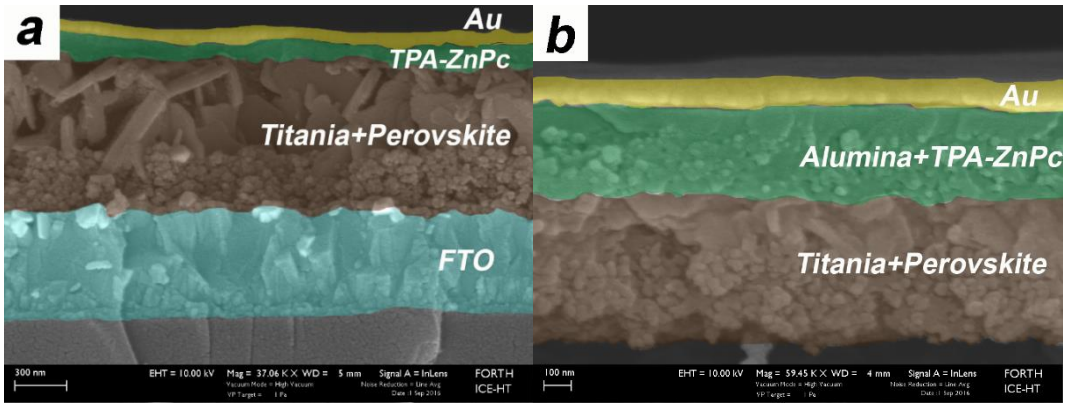

Figure 2. *Cross-sectional FESEM images of the subsequent layers of PSC devices (a) without Al_2O_3 buffer layer; (b) with Al_2O_3 buffer layer. The scale bars correspond to 300 nm (a) and 100 nm(b).*

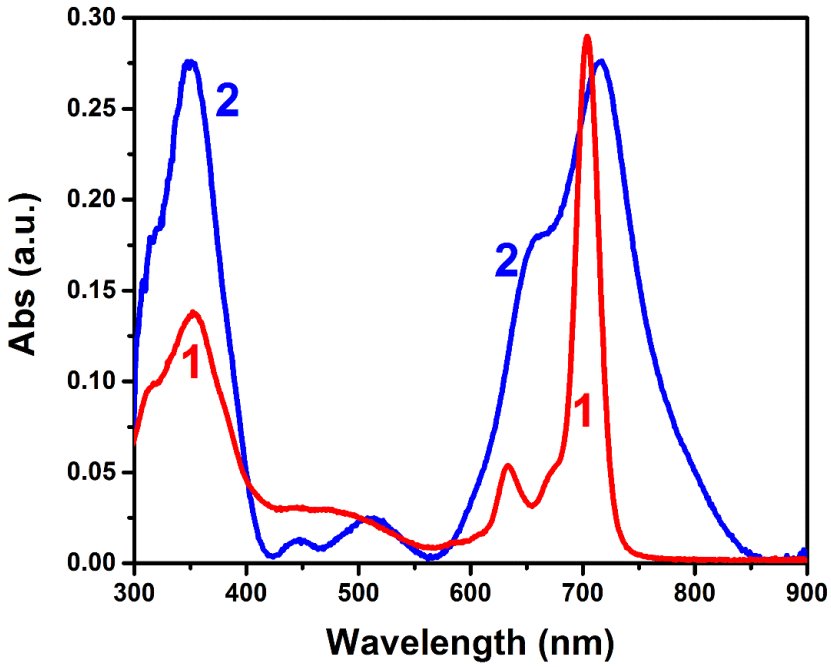

Figure 3. *Absorption spectra of: (1) a dilute solution of TPA-ZnPc in chlorobenzene; (2) a thin film formed by spin coating of TPA-ZnPc on FTO glass.*

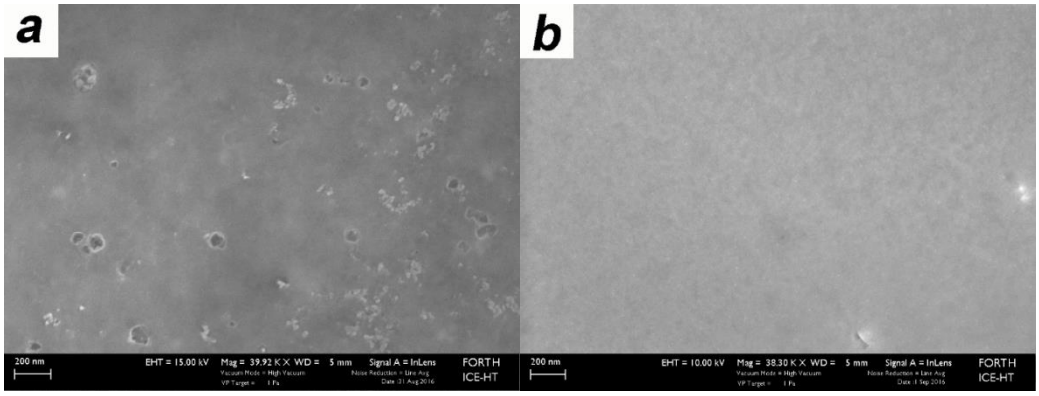

Figure 4. *FESEM top views of TPA-ZnPc films on top of the perovskite layer: (a) without buffer layer and (b) with underlying Al_2O_3 buffer layer. The scale bars are 200 nm.*

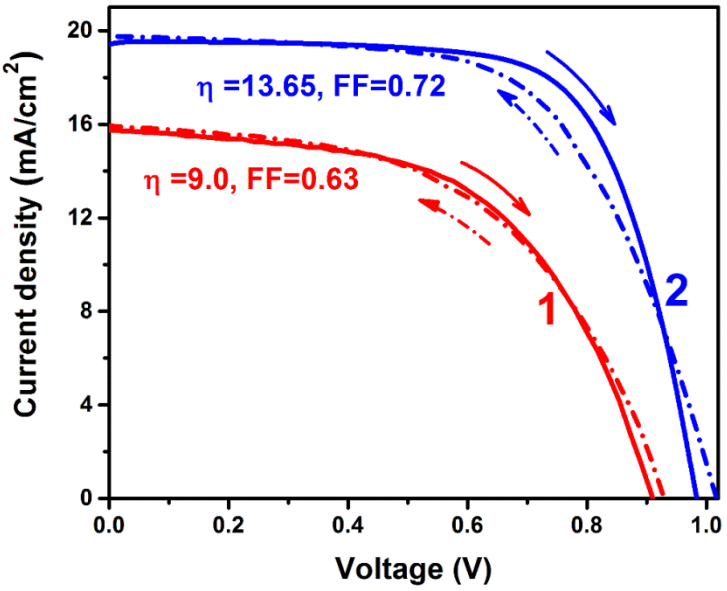

Figure 5. *Current-voltage data and hysteresis of PSC devices made by employing TPA-ZnPc as HTM: (1) in the absence and (2) in the presence of Al_2O_3 buffer layer. Calculated fill factor (FF) and efficiency (η) values are inserted in the figure.*

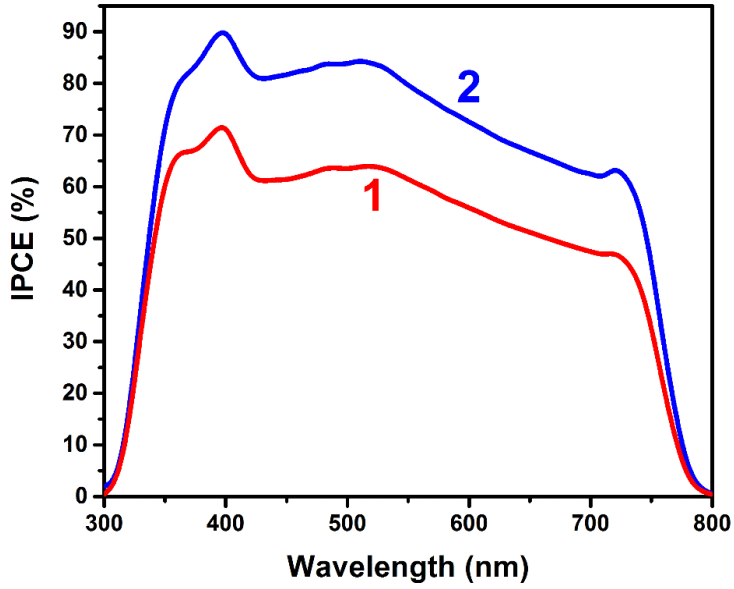

Figure 6*. Action spectra recorded with PSC devices employing TPA-ZnPc as HTM: (1) in the absence and (2) in the presence of* Al_2O_3 *buffer layer.*

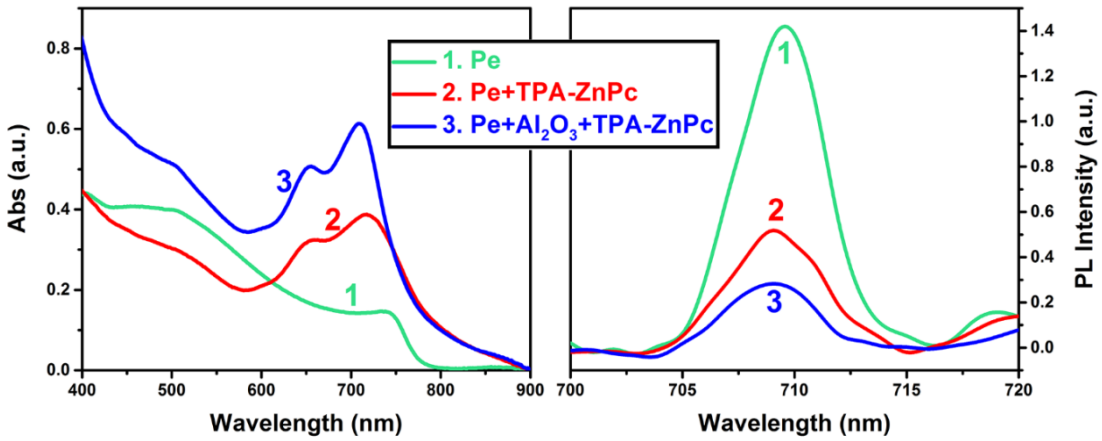

Figure 7. *Absorption (left) and luminescence (right) spectra of perovskite (Pe) films with or without an intermediate buffer layer and a TPA-ZnPc layer on the top: (1) perovskite film alone; (2) TPA-ZnPc/perovskite; (3) TPA-ZnPc/Al_2O_3/perovskite. Photoluminescence was recorded by excitation at 450 nm.*

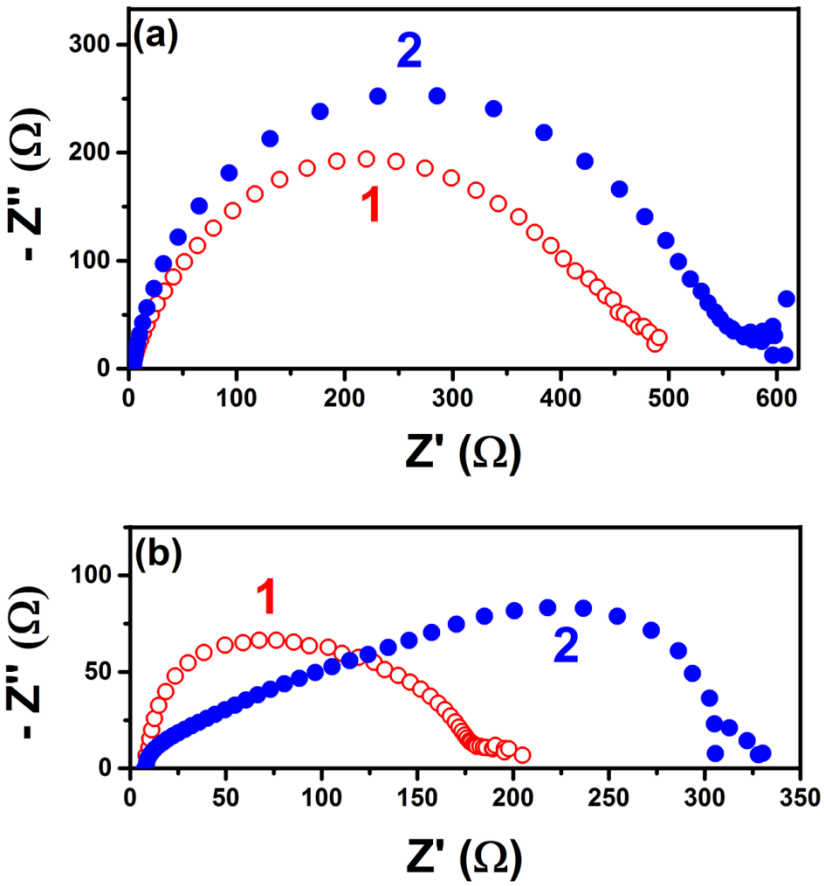

Figure 8. *Nyquist plots traced by applying a voltage equal to V_{OC} under (a) dark and (b) illumination conditions for PSCs employing TPA-ZnPc as HTM : (1) in the absence and (2) in the presence of Al_2O_3 buffer layer.*